High Resolution Triple Axis X-Ray Diffraction Analysis of II-VI Semiconductor Crystals

578-76
039155

H.M. Volz[1] and R.J. Matyi[2]
[1]Materials Science Program
[2]Department of Materials Science & Engineering
University of Wisconsin
1509 University Avenue
Madison, WI 53706
Phone: (608) 263-1716
E-mail: matyi@engr.wisc.edu

The objective of this research program is to develop methods of structural analysis based on high resolution triple axis X-ray diffractometry (HRTXD) and to carry out detailed studies of defect distributions in crystals grown in both microgravity and ground-based environments.

HRTXD represents a modification of the widely used double axis X-ray rocking curve method for the characterization of grown-in defects in nearly perfect crystals. In a double axis rocking curve experiment, the sample is illuminated by a monochromatic X-ray beam and the diffracted intensity is recorded by a fixed, wide-open detector. The intensity diffracted by the sample is then monitored as the sample is rotated through the Bragg reflection condition. The breadth of the peak, which is often reported as the full angular width at half the maximum intensity (FWHM), is used an indicator of the amount of defects in the sample.

In HRTXD, both the incident and the diffracted X-ray beams are conditioned by highly perfect (and typically multiple reflection) X-ray optics to reduce the angular and spectral divergences in both beams. The importance of this arrangement can be appreciated by considering the effect of structural defects on the diffraction process. Compositional variations and/or strains in the crystal lattice will locally change the lattice parameter and will be manifested in variations from the exact Bragg condition in a direction perpendicular to the lattice planes. In contrast, the presence of a mosaic spread in the sample or local angular distortions in the diffracting planes will alter the angular position at which a misoriented region of a crystal diffracts. This effect will be manifested as redistribution of the diffracted intensity in a direction that is parallel to the reflecting planes. By conditioning the incident and diffracted X-ray beams in both angle and wavelength in a HRTXD experiment, the strong, perfect-crystal contribution to the Bragg reflection peak can be discriminated from the weaker, off-peak scatter generated by structural defects. This allows the scattering from defects to be measured directly. HRTXD also has the advantage that it can be applied to crystals with very high defect densities, unlike other methods such as transmission electron microscopy and X-ray topography.

The resulting HRTXD data are commonly plotted as equal-intensity contours as a function of parallel and perpendicular deviations from the exact Bragg condition. These so-called "reciprocal space maps" permit an assessment of the nature and density of the structural defects in the diffracting crystal to be determined either by visual examination or more quantitatively by modeling from diffraction theory. This approach is highly relevant to microgravity research

because it aids in the development of our understanding of the effects of microgravity on crystal growth and the incorporation of defects.

In the present work we have analyzed the defect structures in crystals of ZnSe, $Hg_{1-x}Cd_xTe$, and $Hg_{1-x}Zn_xSe$ that were grown at the Marshall Space Flight Center. Our principal results may be summarized as follows:

ZnSe:

We have performed detailed analyses of four ZnSe crystals (ZnSe-32, -34, -37, and -43) that were grown by physical vapor transport (PVT) at the Marshall Space Flight Center by Dr. Ching-Hua Su. In general, PVT ZnSe crystals showed moderate to extensive diffuse scatter off the main Bragg peak, indicating the presence of grown-in defects. In virtually all cases the extent of the diffuse scatter was much greater than is usually observed in semiconductors such as GaAs or CdTe, suggesting that the grown-in defect density in ZnSe is greater than that seen in these more established materials.

ZnSe-34H: Figure 1 illustrates a high resolution triple axis reciprocal space map recorded from a (220) growth facet on this crystal. This particular reciprocal space map is typical of ZnSe crystals and shows many of the features seen in other crystals. The data are plotted as contours of constant values of the logarithm of the diffracted intensity. The minimum contour level, located furthest from the exact Bragg condition (q_x=q_z=0), is one (or 10^0) counts per second. The data are plotted in steps of $10^{0.25}$ (*i.e.* four contours per decade of intensity). The most notable feature in the plot is the extensive diffuse scatter that radiates away from the exact Bragg condition; this diffuse intensity arises from the long-range strain fields due to defects (primarily dislocations) in the crystal. In addition, a "surface streak" perpendicular to the (220) diffracting planes is also present, which is consistent both with relatively good structural perfection and a smooth surface.

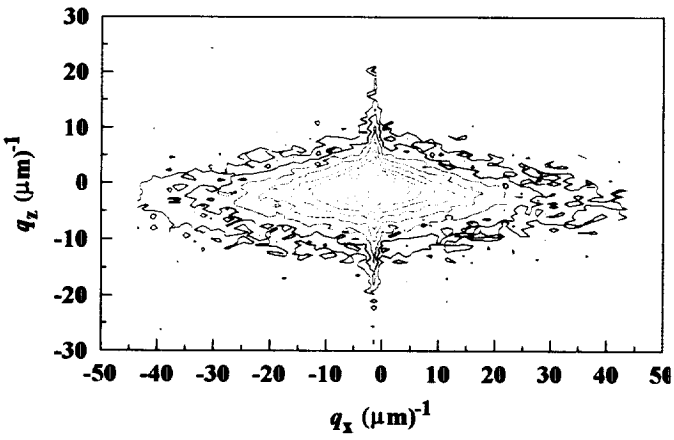

Figure 1. 220 reciprocal space map from ZnSe-34.

ZnSe-32V: A cleaved (220) wafer from crystal ZnSe-32V was examined at different locations to observe spatial variations in the defect structure. Figure 2a (next page) shows the reciprocal space map recorded when the incident X-ray beam illuminated the center of the ~10mm diameter wafer. The data suggest that the center of this particular sample possesses a surprisingly high level of structural perfection; both the intense and well-defined surface streak, combined with a low level of off-peak diffuse scatter, suggests a defect density that is comparable to high quality CdTe or moderate quality GaAs. However, when the X-ray beam was translated 5mm to the wafer periphery, the reciprocal space map shown in Figure 2b was obtained. These data show multiple diffracting regions of low structural perfection, in which the angular range of the scan

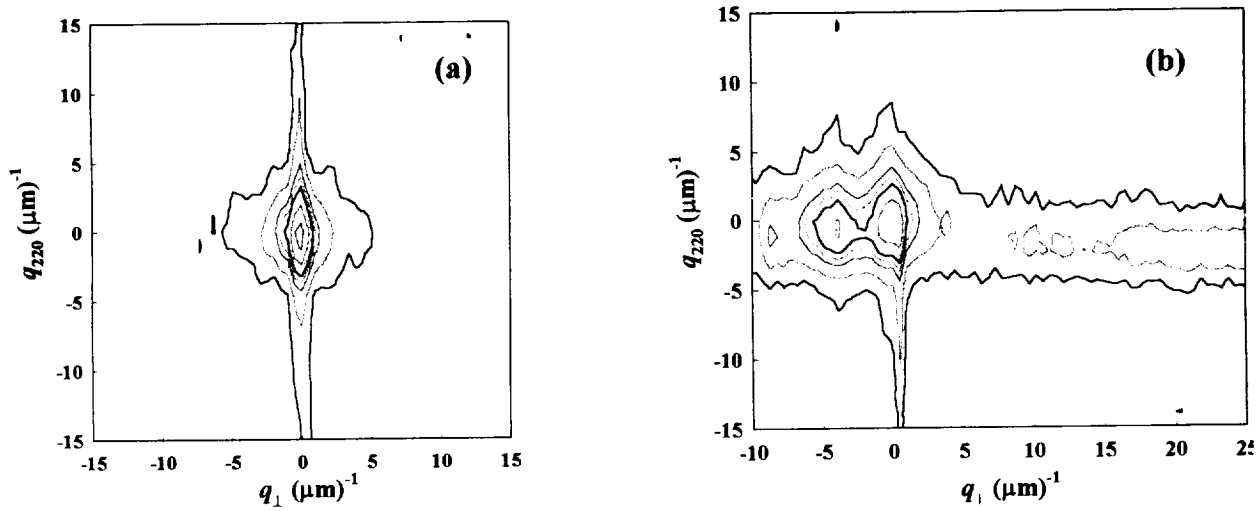

Figure 2. 220 reciprocal space maps from ZnSe-32V. (a) wafer center (b) wafer edge.

(about 0.5°) is consistent with large localized misorientations in the crystal. This interpretation is supported by synchrotron X-ray topographs recorded from this same sample by Prof. M. Dudley at SUNY -Stony Brook[1].

ZnSe-32H: Similar to ZnSe-32V, reciprocal space maps were recorded from different locations on a chemical -mechanical polished (111) wafer prepared from ZnSe-32H. In this case, the different positions were chosen to investigate the possible effect of the gravity vector on the resultant grown-in defect structure. Figures 3a and 3b show (111) reciprocal space maps that were recorded 3mm apart on the crystal surface, corresponding to data from opposite ends of the gravity vector (shown pointing towards the bottom of the page). A quantitative difference in the magnitude of the diffuse scatter from defects is evident, with the ZnSe at the bottom of the gravity vector clearly containing more of this scatter than the crystal at the top of the vector. Unfortunately, the structural perfection of the crystal is rather poor, and it is not possible to determine if the observed scattering is due to intrinsic (grown-in) defects, or if it arose from surface damage caused by the chemical-mechanical polishing process. Further work is needed to more fully resolve this issue.

ZnSe-43H: This single crystal boule had a sufficiently large growth facet to permit *x-y* spatial mapping with both double axis rocking curves and

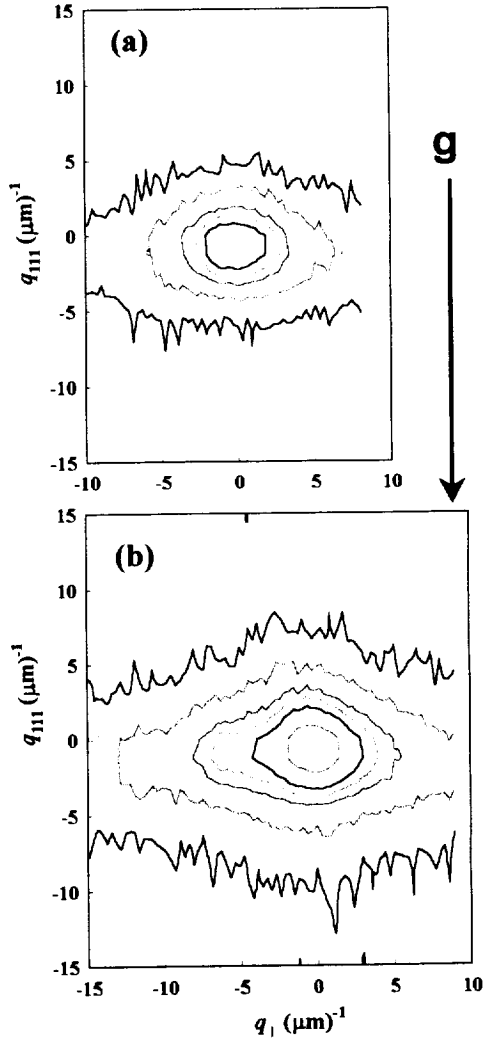

Figure 3. Reciprocal space maps from ZnSe-37. (a) top **g**; (b) bottom **g**.

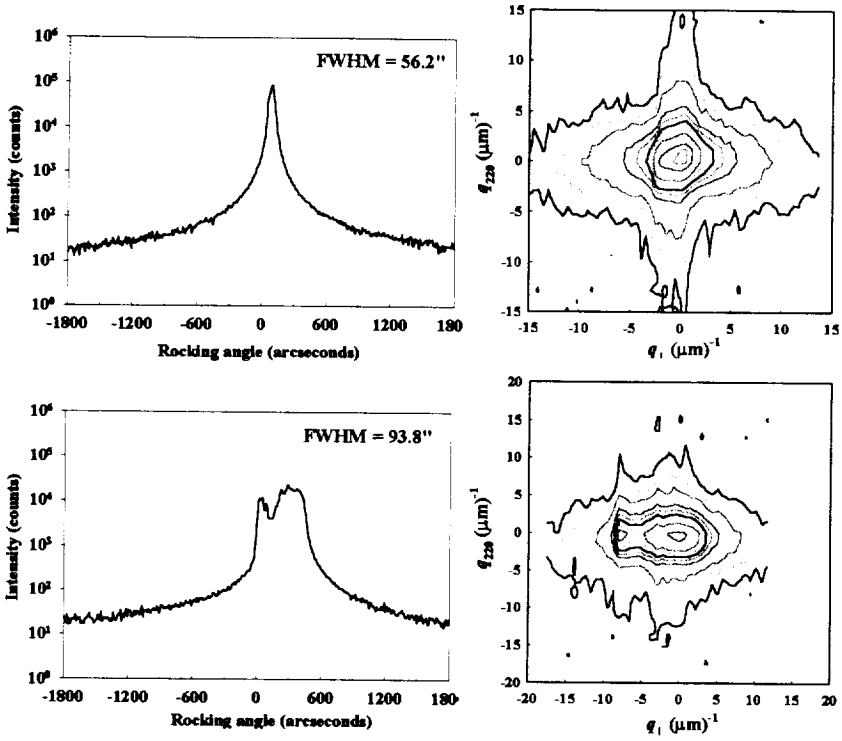

Figure 4. Rocking curves and triple axis reciprocal space maps from ZnSe-43H (see text below for details).

triple axis reciprocal space maps. Figure 4 illustrates data that were recorded at opposite ends of the (220) facet. The top pair (rocking curve and map) were recorded from a position near one edge of the facet; the bottom pair were recorded from the opposite side, about 10mm away. Synchrotron X-ray topographs recorded by M. Dudley[1] showed that the top pair were taken near an inclusion in the crystal, while the bottom pair came from a twinned region. Significant variations between the two regions are obvious. The strain field from an inclusion will broaden the reflection range (thus enlarging the rocking curve FWHM) and will generate off-peak diffuse scatter, but it should not grossly degrade the long-range structural order of the crystal. As a result, dynamical diffraction can occur as is seen in the reciprocal space map. In contrast, the presence of twinned regions and twin boundaries can significantly alter the local diffraction characteristics as slight misorientations between the twins, causing them to diffract kinematically. This is precisely what is observed in the reciprocal space map, and it explains the splitting observed in the rocking curve.

$\underline{Hg_{1-x}Cd_xTe}$:

The above analysis illustrates the synergy that exists when high resolution triple axis X-ray diffraction studies are combined with X-ray topography of the same material. A recent analysis

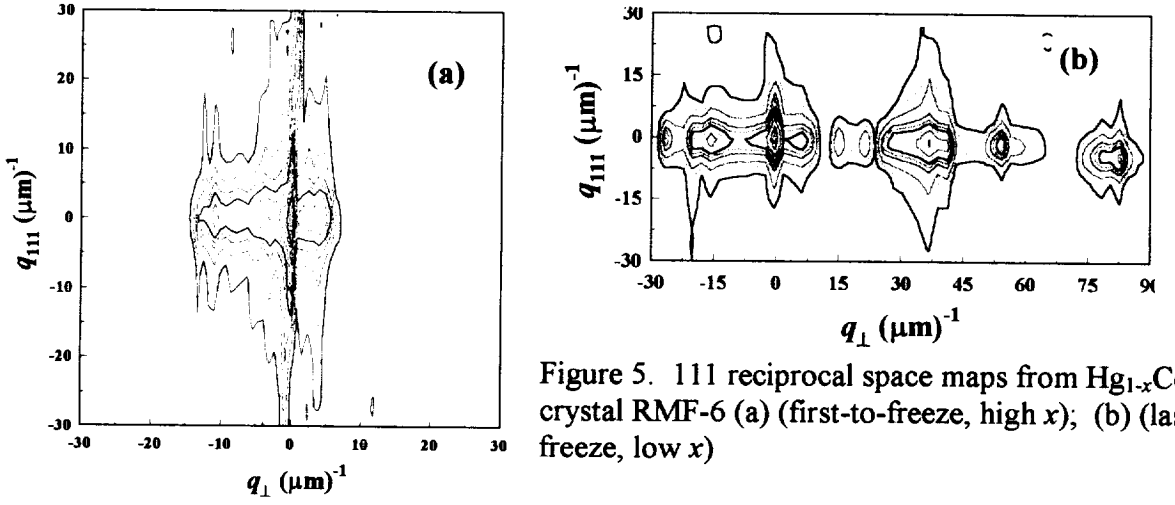

Figure 5. 111 reciprocal space maps from $Hg_{1-x}Cd_xTe$ crystal RMF-6 (a) (first-to-freeze, high x); (b) (last-to-freeze, low x)

of an $Hg_{1-x}Cd_xTe$ crystal grown at MSFC by Dr. D. Gillies by the traveling heater method from a tellurium zone further illustrates this fact. Figure 5a shows the reciprocal space maps that were recorded from the first-to-freeze (high x, low % Hg) and last-to freeze (low x, high % Hg) ends of the THM crystal. In the first-to-freeze material, the mosaic blocks are large enough to diffract dynamically, as illustrated by multiple surface streaks. This is not the case in the last-to-freeze material, Figure 5b. The mosaic spread is extremely large (note scale), with discrete mosaic blocks that approach polycrystallinity. Within each block, little evidence of a surface streak can be observed, suggesting a low degree of structural perfection. These results were confirmed by data collected from topographs recorded from adjacent samples[1].

One of the principal goals of this investigation was to see if the application of a magnetic field could reduce the density of grown-in defects. Figure 6 illustrates (111) reciprocal space maps from similar first-to-freeze and last-to-freeze sections of a $Hg_{1-x}Cd_xTe$ crystal grown with magnetic assistance. A casual examination of the reciprocal space maps reveals a significant reduction in the defect density of the crystal; in fact, the first-to-freeze region looks quite similar to what one would expect to see from nominally high quality CdTe. Although the defect density of the last-to-freeze sample was inferior to the first-to-freeze material, comparison with Figure 5b indicates that the application of the magnetic field during growth lowered the defect density in the last-to-freeze material by many orders of magnitude. All of these conclusions agree fully with those made from topographic analyses.

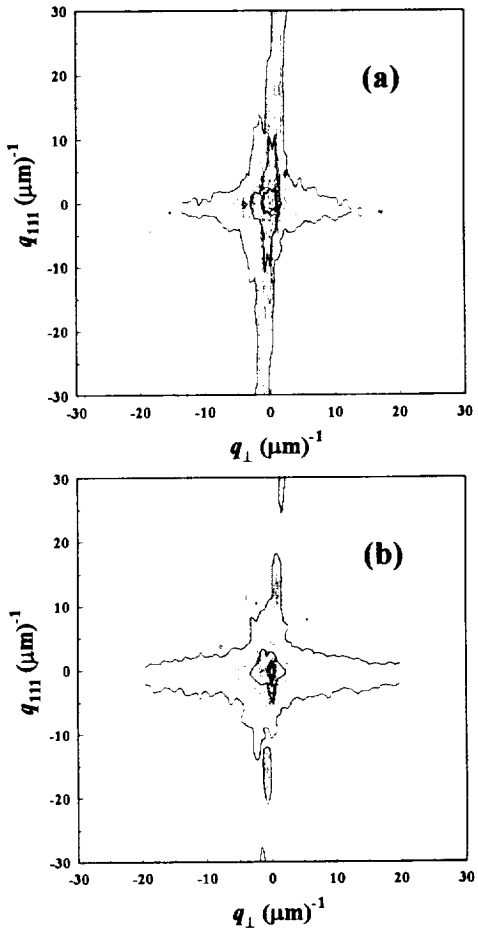

Figure 6. 111 reciprocal space maps from $Hg_{1-x}Cd_xTe$ crystal RMF-7 (a) (first-to-freeze, high x); (b) (last-to-freeze, low x)

<u>$Hg_{1-x}Zn_xSe$</u>:

Finally, a high resolution X-ray diffraction analysis has been performed on a $Hg_{1-x}Zn_xSe$ ($x \approx 0.1$) crystal grown by the Bridgman method by Dr. Su at MSFC. The (111) double axis rocking curve shown in Figure 7 exhibits multiple peaks, thus indicating a highly mosaic structure. However, it is not possible to infer much additional information from this one curve. In contrast, the triple axis reciprocal space map of the (111) reflection conveys much more. The breadth of the mosaic spread and the overall level of structural imperfection is clearly seen in the triple axis data. Somewhat surprisingly, etch pit density measurements of the defect density of this crystal returned estimates that ranged from 1×10^5 cm^{-2} to 9×10^3 cm^{-2}. These values seem extremely low given the appearance of the reciprocal space map. Possible reasons for this discrepancy are currently under investigation.

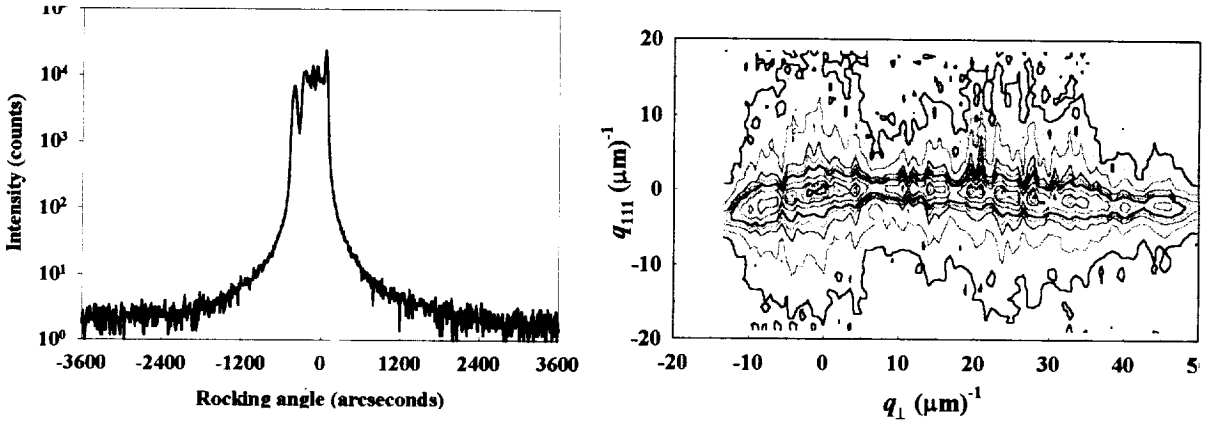

Figure 7. (111) double axis rocking curve (left) and triple axis reciprocal space map (right) from $Hg_{1-x}Zn_xSe$.

The reciprocal space map from the $Hg_{1-x}Zn_xSe$ also shows a systematic change in lattice parameter (presumably due to changes in the mercury content) as a function of angular deviation from the mean Bragg position. A calculation based on the maximum and minimum values of q_{111} in Figure 7 reveals that a 2% variation in Hg-content across the irradiated volume could account for the observed behavior. However, the reciprocal space map also suggests a possible correlation between defect structure and chemical composition of the crystal. Work is in progress to more fully understand this observation.

In conclusion, this work has shown that high resolution triple axis X-ray diffraction is an effective tool for characterizing the defect structure in semiconductor crystals, particularly at high defect densities. Additionally, the technique is complimentary to X-ray topography for defect characterization in crystals.

Acknowledgements:

The authors acknowledge Dr. S.Cobb, Dr. D. Gillies, Dr. S. Feth, and Dr. C-H. Su of the Marshall Space Flight Center for supplying the materials used in this study and for useful discussions. They also acknowledge Prof. M. Dudley (SUNY- Stony Brook) for the synchrotron X-ray topography. This work was supported by NASA under contract NCC8-48 and USRA under contract 3537-08.

References:

1. See M. Dudley and R.J. Matyi, "Combined Synchrotron White Beam X-Ray Topography and High Resolution Triple Axis X-Ray Diffraction Characterization and Analysis of Crystals Grown in Microgravity and Ground-Based Environments," in these proceedings.